# Texture Development in a Cold-Rolled and Annealed Body-Centered-Cubic Mg-Li Alloy

G.J. SHEN and B.J. DUGGAN

The rolling and annealing textures formed in bcc Mg 14 wt pct Li have been investigated and compared with interstitial-free (IF) and more heavily alloyed ferritic steel rolled at the same temperature. The α fiber texture component (<110>//rolling direction) is very strong after 90 pct rolling at room temperature; however, there is evidence that the γ fiber ({111}//rolling plane) weakens with increasing rolling strain to give a peaklike texture centered on {111}<110>. A rarely found cold rolling fiber texture has been identified, which has {100}//rolling plane and peaks at {100}<014>. Annealing at 200 °C very rapidly produces {554}<225>, which gives way to components near {111}<123> on grain growth. The α fiber is destroyed by recrystallization; however, the {100}//rolling plane fiber shifts intensity from the as-rolled orientation {100}<014> to {100}<012>. Since texture largely determines drawability, the best that can be achieved in terms of press performance of this alloy is most likely a Lankford parameter of unity.

## I. INTRODUCTION

THE reduction of the weight of vehicles used for land transportation is essential if increasingly strict constraints on combustion products are to be met. However, despite being relatively heavy, the press performance of bcc interstitial-free (IF) steel in making automobile body panels is unmatched by any other material of the same cost. Good press performance requires a high work hardening rate in order to guard against diffuse necking in any element of a pressing that is subject to stretching and a high Lankford parameter (the width-to-thickness strain at a certain elongation in a conventional tensile test of the sheet), which ensures deep drawability. The work hardening rate in IF steel is moderate. The bcc lattice does not work harden as rapidly as an fcc lattice, due to the abundance of slip systems in bcc systems and the ease of cross-slip. However, the drawability is far higher than in fcc materials. It is relatively easy, using conventional rolling and annealing plants, to obtain IF steel with Lankford parameters on the order of 2.0, while aluminum, a possible substitute material, has a Lankford parameter of 0.5 to 0.7 in conventional alloys. The Lankford parameter depends on the texture of the material and is equal to unity for a randomly textured material. Any number above unity is desirable for deep drawing, which provides the impetus for this research since it is known that, when Mg is alloyed with Li and the alloy level reaches ~30 at. pct (~10 wt pct), the lattice transforms to

bcc (β phase) from the hcp (α phase).[1] With the addition of aluminum, an alloy LA141 (Mg-14 pct Li-1 pct Al) and a density of 1350 kg/m$^3$ is among the lightest of metals possessing useful strength, and can be used as armor plate and in the aerospace industry.[2]

Since this article describes the formation of rolling textures, and a heavily alloyed material is involved, the question of the stacking fault energy (SFE) of the lattice must be addressed. This is not a straightforward process, since there is no such information in the literature and it has proved impossible to image a foil in a transmission electron microscope due to the extreme reactivity of this material's surface. However, it is vitally important to consider SFE due to its known effect on the rolling textures of cubic fcc metals and alloys. For fcc, it is known that alloying affects the SFE, and there are characteristic textures associated with materials of high and low values of SFE. For example, Cu, an intermediate to high SFE material, produces what is known as a Cu-type texture. However, alloying with Zn to 30 pct produces the Brass-type texture. There is good reason to associate the transition from Cu-type to Brass-type textures as SFE is reduced by the alloying, with ease of cross-slip.[3,4] Homologous temperature is also a key factor, since low-temperature rolling of Cu produces a brass-type texture and high-temperature rolling of α brass produces a Cu-type texture.[5] Again, the transition is associated with ease of cross-slip. The last exhaustive review in English of bcc alloy rolling texture was done ~40 years ago by Dillamore and Roberts,[6] who reported that rolling textures in Mo-35 pct Re, Co 50 pct Fe 48 pct V 2 pct, metastable ZrNb, and Fe-3 pct Si all produced very similar rolling textures to those found in relatively pure Fe, which is a metal of high SFE. More recent work using higher resolution techniques based on the orientation distribution functions (ODFs) has shown that ferritic stainless steel (Fe-10 pct-16 pct Cr)[7] and Fe 3 pct Si[8] produce rolling textures

G.J. SHEN, Professor, is with the South East University, Nanjing, China. B.J. DUGGAN, Professor, is with the Department of Mechanical Engineering, The University of Hong Kong, Pokfulam Road, Hong Kong, Hong Kong. Contact e-mail: bjduggan@hkucc.hku.hk

identical to those produced in low C and IF steels.[9] These results indicate that alloying different metallic elements that form bcc structures to the levels investigated does not produce texture modifications, which can be attributed to a lowering of their SFEs. However, no articles deal with bcc MgLi from a texture standpoint; thus, another approach is to consider the mechanical properties of the material. It is well known that the toughness of bcc metals and alloys as measured in impact tests is a function of temperature of testing. It is also known that the flow stress is also a function of temperature, increasing as temperature reduces. These changes from tough to brittle behavior and increasing strength are related to the dislocation cores and the ease of kink pair formation cores of screw dislocations in the bcc lattice, with cross-slip being relatively easy at temperatures close to room temperature in relatively pure Fe and Mo, but relatively difficult at lower temperatures. These results indicate that alloying different metallic elements that form bcc structures to the levels investigated does not produce texture modifications that can be attributed to a lowering of their SFEs. A similar variation in flow strength has been found in bcc MgLi. Saka and Taylor[10] showed that various orientations of bcc single crystals yield stress at 20 K decreased from 100 to 30 $\text{MNm}^{-2}$ at ~300 K. Over the temperature range 77 to 300 K, pure iron decreased in yield stress from 400 to 50 $\text{MNm}^{-2}$.[11] In the case of Fe, there was strong evidence for slip to concentrate on the 110 slip system at 77 K; however, this was not found in bcc MgLi since the glide bands were determined by the maximum shear stress plane as temperature increased from 4 to 77 K.[10] Polyslip was inferred and was used to explain the observation that bcc MgLi is not brittle, even at 4.2 K. Russell *et al.*[12] postulated that, in this system, the critical resolved shear stresses for the 110, 112, and 123 slip systems are nearly equal, which prevents pileups producing crack nuclei since cross-slip would be easy. This ease of cross-slip indicates that bcc MgLi is a material of highly effective SFE, even though the alloy level is very significant (35 at. pct) and can be legitimately compared in its rolling texture behavior with other bcc metals and alloys. Hence, rolling textures are presented and discussed in light of the extensive literature concerning relatively pure Fe and IF steel, and, where appropriate, ferritic stainless steel and Fe-3 pct Si. Furthermore, because of this similarity, the annealing textures are also compared with ferritic alloys.

## II. EXPERIMENTAL

A bcc alloy of Mg 14 wt pct Li was prepared by casting and homogenization at 623 K for 24 hours at the Institute for Corrosion and Protection of Metals (Shenyang, China). To produce a suitable geometry for rolling, and to destroy the cast structure, the material was pressed to form a rod shape at 573 K and then subject to equal channel angular processing (ECAP) at 400 K using an MTS800 machine with an angle of 90 deg. Four passes were used before rolling at 473 K to produce hot band 1.6-mm thick and ~10-cm wide. This was divided into two batches, one used in the as-received condition and the other annealed at 200 °C (0.55 $Tm$, where $Tm$ is the absolute melting temperature) to remove the warm-rolled structure and texture. The materials were then rolled at ~10 pct reduction per pass to ensure homogeneous deformation at room temperature (0.35 $Tm$) up to a maximum reduction of 90 pct. Annealing was done in an oil bath maintained at 200 °C. Pole figures were determined by the reflection method using Cu $K_\alpha$ radiation and the ODFs calculated from the 110, 200, and 211 pole figures using the BATE software.

Metallography proved exceedingly difficult with this alloy, since the freshly exposed surfaces degraded within a few seconds of exposure to the air. A total of five different laboratories were consulted to find a solution to this problem without success. Professor Shig Saimato, Queens University (Kingston, Ontario, Canada), made the crucial recommendation to use paraffin both as a lubricant for mechanical polishing and storage of the material before and after electropolishing. The most successful polishing solution was ice cold 1:3 HCl/ethanol. The samples were immersed in Analar paraffin for storage after mechanical and electropolishing. A LEO S360 scanning electron microscope (SEM) was used for examination of the surfaces using a backscattered detector with a minimum exposure to air during loading into the SEM (CAMBRIDGE S360). Hardness measurements were standard, and at least 30 measurements were made for each thermally-equilibrated condition.

## III. RESULTS

### A. *Cold Rolling*

The as-received hot band had an elongated grain structure ~80-$\mu$m thick and ~120-$\mu$m long. Highly reactive particles were etched out at some of the grain boundaries and these particles are of unknown chemistry. Complete annealing of the hot band produced the microstructure shown in Figure 1(a), which is from the rolling plane (RP) section. The grains revealed a range in size from 50 to 120 $\mu$m with an average diameter of ~100 $\mu$m, after annealing at 200 °C for 15 minutes. The ODFs and 200 pole figures for the as-received and annealed hot band are shown in Figures 1(b) and (c). Also included is a labeled $\phi_2$ 45 deg section of Bunge's[9] version of Euler space (Figure 1(d)). The $\alpha$ and $\gamma$ fibers are indicated. As expected, the well-defined $\alpha$ and $\gamma$ fibers formed during the final low-temperature pass during warm rolling (Figure 1(b)) were weakened by the annealing (Figure 1(c)).

Cold rolling the as-received material 37, 73, and 90 pct produced the textures shown in Figure 2, along with their corresponding 200 pole figures. The strengthening of the $\alpha$ fiber is remarkable, as is the fact that it weakens steeply as {111} <110> is approached. The $\gamma$ fiber appears to be destroyed as rolling reduction increases. All that is formed belonging to this fiber is the near {111} <110> component, an orientation common to both the $\alpha$ and $\gamma$ fibers. Also present is another fiber texture, which has {100} parallel to the rolling
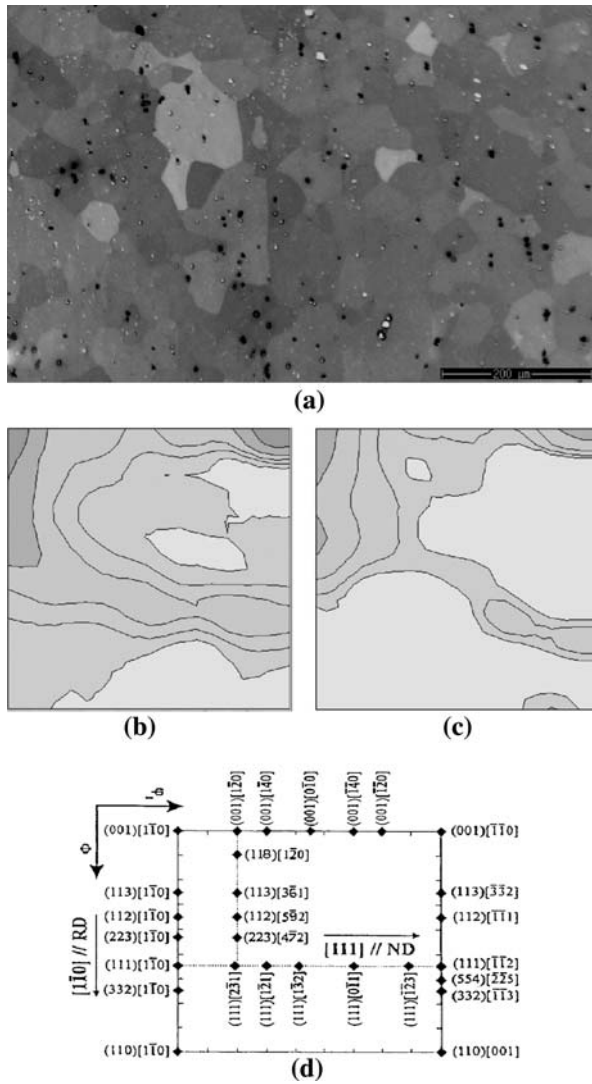
Fig. 1—(a) SEM channeling and secondary electron contrast micrograph of the annealed hot band. (b) $\phi_2$ 45 deg section of the complete ODF of the as-received hot band. (c) Same section of the ODF for the annealed hot band. (d) Fully labeled $\phi_2$ 45 deg section showing the important orientations. The $\alpha$ and $\gamma$ fiber textures are indicated in (d).

plane and includes {100}<011> (a point common to both the $\alpha$ fiber and this third fiber), which will be designated the {100}//RP fiber. A similar fiber was designated by Mishra et al.[8] as the v fiber. There are quite clearly subsidiary peaks near the {100}<014> positions (Figure 1(d)).

Annealing the hot band at 200 °C produces very little change in texture, as observed by comparing Figures 1(b) and (c). Cold rolling this annealed material to the same level of reduction produces the textures shown in Figure 3. Again, the similarities between the cold rolling textures formed in the two starting materials are obvious, although when Figures 2 and 3 are compared, it must be noted that the intensities are lower. In addition, the main difference is that there is a discernible $\gamma$ fiber in Figure 3, which is almost absent in Figure 2, and there are no {100}<014> peak components in the {100}//RP fiber.

Figure 4 shows an SEM micrograph after 73 pct cold rolling of the annealed hot band, and it is clear that shear banding is occurring in some crystals. These shear bands are found in both of the cold-rolled starting materials and increase in number as cold rolling increases from 73 to 90 pct. These shear bands appear to be similar to those observed in IF, ferritic stainless, and electrical IF steels and are not observed to cross grain boundaries at 90 pct reduction, nor are they found in all crystals.

### B. Recrystallization Behavior

The softening curves at 200 °C for the as-received and cold-rolled hot band, and for the annealed and cold-rolled hot band, are shown in Figures 5(a) and (b), respectively. Also shown is the behavior of the hot band under identical conditions, which falls from the as-received value of 60 to 46 VHN (Figure 5(a)) and remains at this lower value with prolonged heating (Figure 5(b)). Annealing of all of the deformed materials, independent of cold rolling degree, shows hardness falling from initial values of 62 to 65 VHN to levels of 46 to 54 VHN, except for the cold-rolled 90 pct as-received hot band, which declines to a higher value of 58 VHN. Clearly, with such small variations in hardness from the as-rolled to the fully annealed states, it is not possible to estimate the degree of recrystallization with any certainty from the hardness results. Instead, the SEM was used to determine the degree of recrystallization. As an example of this procedure, Figures 6(a) through (c) show partial recrystallization in the annealed hot band after 37, 73, and 90 pct cold rolling and 200 °C exposure. From these results, it was possible to construct Figure 7, which shows typical kinetics for material after heavy rolling. Given the difficulty of metallography, the only curve that could be measured with certainty was that for the 90 pct cold-rolled material. However, this research established that, for the 37 and 73 pct cold-rolled material, the time for complete recrystallization was less than 200 seconds for both the as-received and annealed hot band starting materials.

The texture changes as recrystallization proceeds at 200 °C in the annealed hot band cold-rolled 90 pct are shown in Figure 8, along with a $\phi_2$ 45 deg ODF section showing the key orientations associated with the recrystallization textures. These changes are very similar to those found in the similarly treated as-received condition. The $\gamma$ fiber weakens as recrystallization occurs, and a component near {554}<225> appears at about 50 pct volume fraction recrystallized (after 60 seconds), and this increases in strength when recrystallization is complete after 180 seconds at 200 °C (Figure 8(e)). Figure 5(b) shows that this texture change from the typical as-rolled bcc type to a mixture of {544}<225> and near {100}<012> components has occurred with only a small change in hardness, i.e., from an initial value of 67 to 59 VHN. Prolonged holding at 200 °C reduces the hardness from its fully recrystallized value of 59 to 53 VHN. In the overall changes in hardness, both of these relative differences are significant. Material was
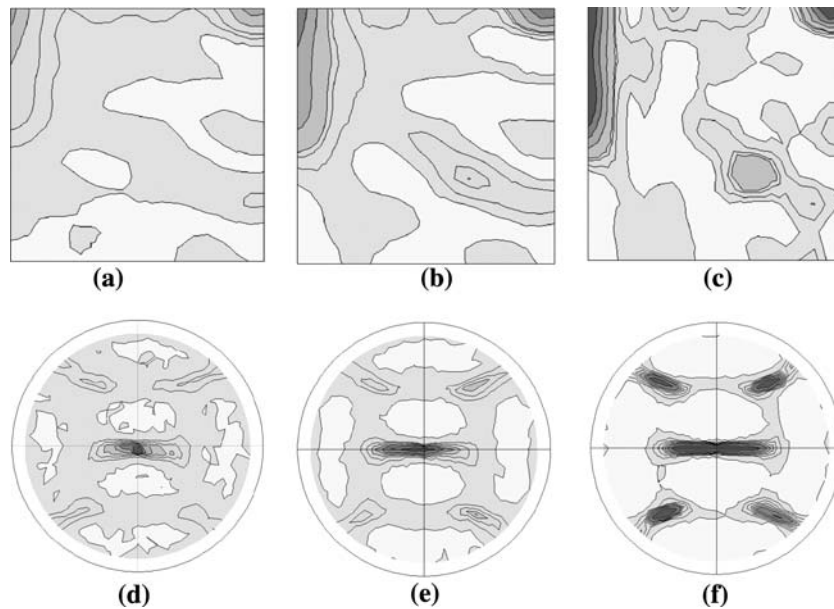
Fig. 2—$\phi_2$ 45 deg ODF section showing the development of texture with increasing rolling reductions of the as-received hot band, along with their respective 200 pole figures. The ODF indexing refers to the $\phi_2$ 45 deg section in Fig. 1(d). Contours: 0, 2, 4, 6, 8, 10, and 14 times random.
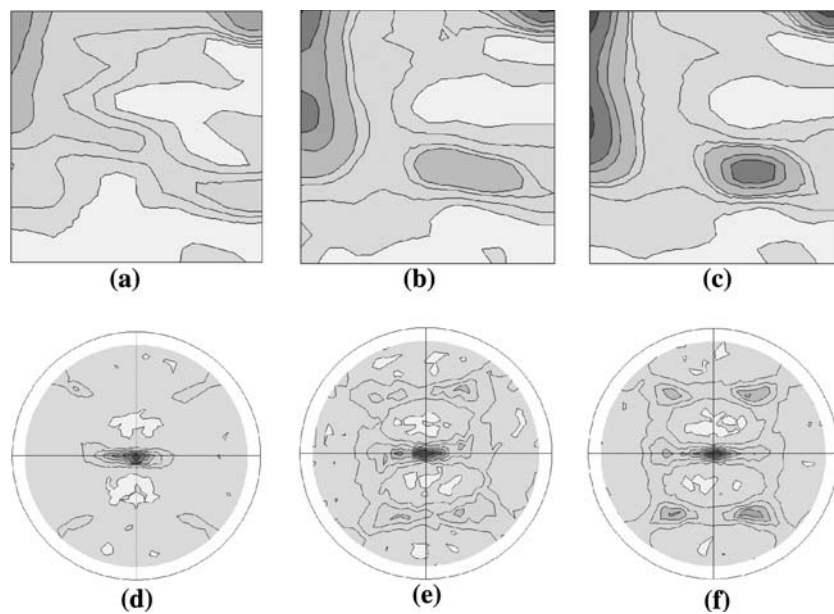


Fig. 3—$\phi_2$ 45 deg ODF sections showing the development of texture with increasing rolling reductions of the annealed hot band, along with their respective 200 pole figures. The ODF indexing refers to the $\phi_2$ 45 deg section in Fig. 1(d). Contours: 0, 1, 2, 3, 4, 5, and 6 times random.

therefore further annealed for a total of 15 minutes when the hardness was approaching its steady value, and the textures measured are shown in Figure 9 for both the as-received and annealed hot bands. Dealing first with the as-received, cold-rolled, and annealed material (Figures 9(a) through (c)), the trends with increased rolling reduction are the same. There is a relatively flat texture after 37 pct rolling, and the higher rolling strains have the same components with greater intensity in the 73 and 90 pct material. The $\alpha$ fiber

texture is destroyed, and near {100}<012> components are formed along the {100}//RP fiber, replacing the {100}<014> components. The strength of this component depends on rolling degree, *cf.* Figures 9(a) through (c).

The strongest peaks near the $\gamma$ fiber are located at (557) [27 $\overline{41}$ 10], (111)[1 $\overline{3}$ 2], and (665)[$\overline{10}$ $\overline{25}$ 42]. These orientations are 9.8, 0, and 4.95 deg, respectively, from the closest {111}<123> positions (Figure 1(d)), and for ease of description will be
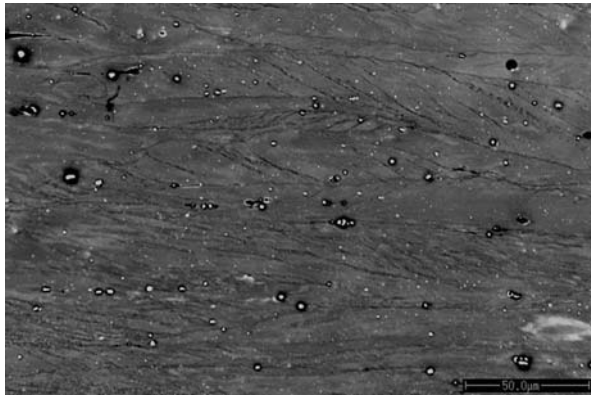
Fig. 4—Channeling + secondary electron contrast micrographs of material rolled at room temperature to 73 pct.
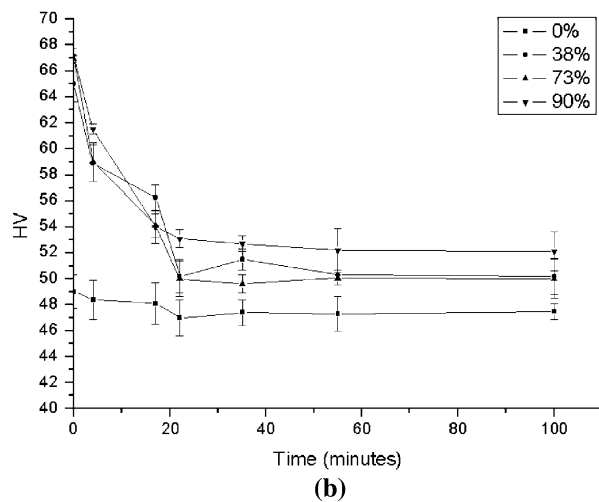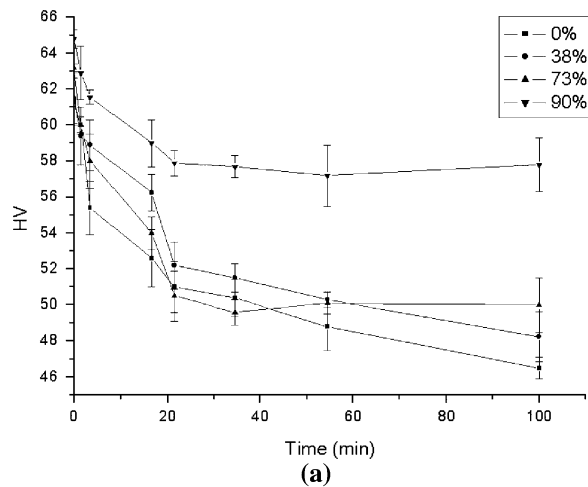




Fig. 5—Softening curves of material rolled to different degrees. (*a*) As-received hot band and (*b*) annealed hot band. In all cases, the annealing was done in an oil bath maintained at 200 °C.



Fig. 6—Channeling + secondary electron contrast micrographs of material cold rolled (*a*) 37 pct, (*b*) 73 pct, and (*c*) 90 pct and annealed at 200 °C for 30 s in an oil bath.

ities with those shown in Figures 9(a) through (c), with the intensities being somewhat lower in the annealed hot band. This is expected, since the hot band was already in possession of a weak rolling texture and, presumably, a deformed microstructure remained from the warm rolling. Thus, the effective rolling strain in the hot band would be higher than in the annealed hot band, which would then influence the recrystallization and the growth textures at the same nominal strain.

described as "near {111} < 123 >" components in general discussion.

The effects of annealing the hot band before cold rolling on the recrystallization textures are shown in Figures 9(d) through (f), and there are marked similar-
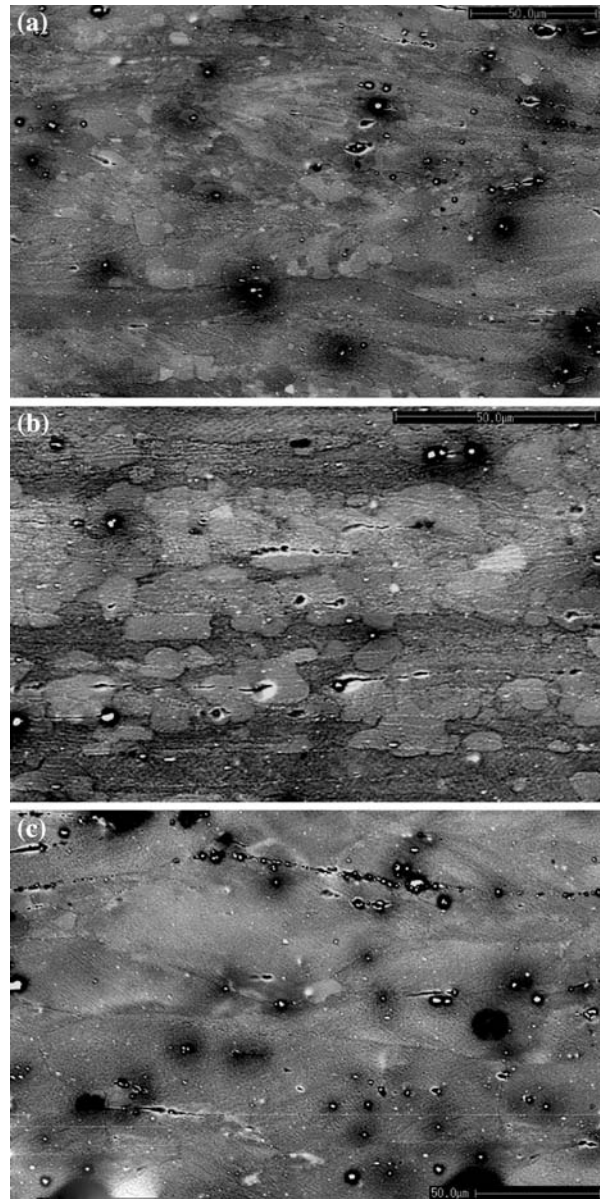
## IV. DISCUSSION

### A. *Initial and Rolling Textures*

The composition of the alloy and the temperatures used in this research ensured that the material was warm
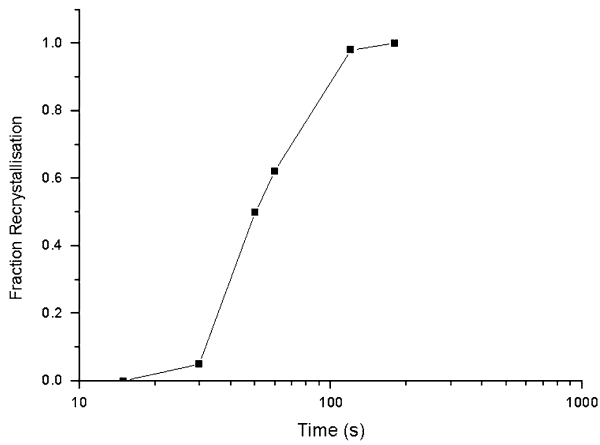
Fig. 7—Annealing kinetics for material cold rolled 90 pct and held for various periods at 200 °C in an oil bath.

rolled in the bcc phase field. Annealing at 200 °C weakened the bcc rolling texture by a recrystallization process, since the only way to significantly change an existing ODF is by the migration of high-angle boundaries, *cf.* Figures 1(b) and (c).

Proper comparison between the bcc MgLi used here and other bcc alloys, such as IF steel, requires the IF steel to have been warm rolled in the bcc phase field rather than the more common method of processing, in which the hot band is rolled in the austenite condition before cooling into the ferrite region for subsequent cold rolling. This is essential because room temperature is 0.35 $Tm$ for this alloy. This has been demonstrated by

Barnett and Jonas,[13] who rolled IF steel in the ferrite phase field up to 700 °C and found an increasing spreading along the {100}//RP fiber from its common point with the α fiber, {100}<011>, toward {100}<001> as rolling temperature increased from 70 °C to 700 °C. Quadir and Duggan[14] repeated this work and found similar results. When ferritic stainless steel (Fe-16.5 pct Cr) was rolled at a temperature that ensured that the material remained in the bcc phase field, it also showed the {100}//RP, although Raabe[15] did not comment on this aspect of his results. Thus, it is concluded that the presence of the {100}//RP fiber appears to be a function of the temperature of rolling, rather than the presence of alloying elements, since both IF steel and ferritic stainless steel both demonstrate a similar tendency to populate this fiber when rolled at elevated temperatures.

Existing "Taylor"-type theories can explain the α and γ fiber components quite well.[16–18] Although the {100}// RP fiber is not predicted, Quadir and Duggan[14] attempted to follow how the α fiber developed in a microstructural investigation of IF steel. Using a high-resolution SEM, they showed that part of the α fiber stretching from {111}<110> to {112}<110> had microstructures comprising microbands aligned at ±20 to 40 deg to rolling direction (RD) when initially formed. From ~{114}<110> to {100}<110>, the microstructure was of very large cells up to moderate cold rolling reductions. However, at cold reductions of ~80 pct of the previously warm-rolled material, there was evidence of orientation splitting in this part of the α fiber. They were able to correlate this behavior with the development of orientations along the α fiber, such as {411}<110> and
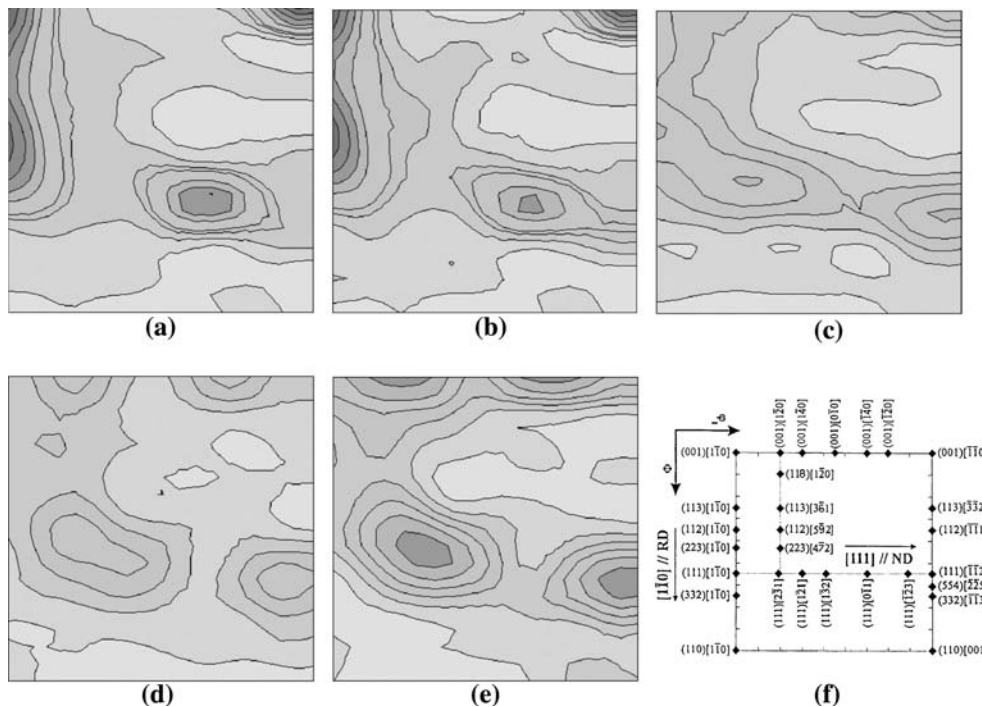


Fig. 8—$\phi_2$ 45 deg sections of the ODFs of annealed hot band cold rolled 90 pct and annealed at 200 °C for (*a*) 0 s, (*b*) 30 s, (*c*) 60 s, (*d*) 120 s, (*e*) 180 s, and (*f*) $\phi_2$ 45 deg ODF section showing the important orientations associated with recrystallization.
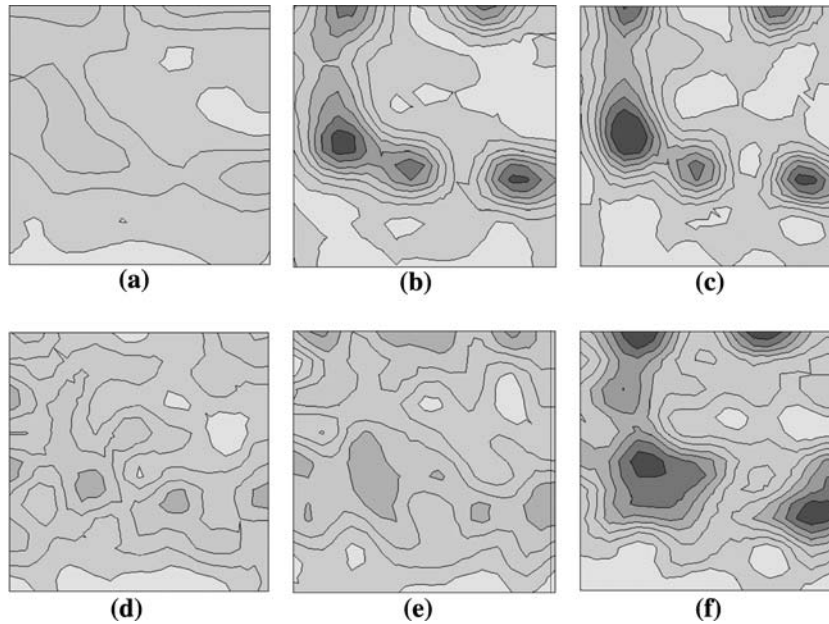
Fig. 9—$\phi_2$ 45 deg sections of the ODFs of materials cold rolled 37, 73, and 90 pct and annealed for 15 min at 200 °C. (a) through (c) From the as-received hot band material and (d) through (e) from the annealed hot band.

also {100}//RP, which could be the origin of the {100}//RP fiber. The peak at {100}<014> is also found in very heavily rolled IF steel, in Fe-3 pct Si (where it is identified as {100}<013>),[8] and the most heavily rolled MgLi investigated here, and most likely originates from orientation splitting of α fiber material.[14]

The micrograph from the longitudinal section (LS) after 73 pct reduction shows narrow shear bands in some grains, which terminate at grain boundaries, making 30 to 40 deg with RD in this section (Figure 4). This micrograph shows many similarities with IF steel rolled to the same degree. There is insufficient material located within the shear bands to affect the rolling texture.

### B. Annealing Studies

Figure 7 shows the recrystallization kinetics for the as-received and cold-rolled 90 pct material at 200 °C. According to this figure, recrystallization was complete after 3 minutes, as it was in all of the samples used here. Inspection of the hardness data in Figure 3 demonstrates a fall between 2 and 10 VHN over the same period, while the ODFs showed major changes. Only migrating high-angle boundaries can change the as-rolled ODFs (Figures 2(c) and 3(c)) to the ODFs for the corresponding materials shown in Figures 8(e) and 9(e). Thus, we have complete recrystallization with almost no softening at this stage.

Figure 8 demonstrates how the recrystallization texture develops in the annealed hot band following cold rolling to 90 pct. The {111}<110> component weakens after 30 seconds at 200 °C (Figure 8(b)), which is followed by the elimination of the α fiber after 60 seconds (Figure 8(c)). At this time, the near {111}<123> components are beginning to form, as are the {100}//RP components. A well-developed texture is formed at

complete recrystallization (Figure 8(e)). Modern explanations for the formation of γ-related texture components on recrystallization, i.e., {554}<225> and {111}<123>, in low-carbon and IF steel are largely based on the oriented nucleation theory.[19] The nucleation sites are assumed to be near grain boundaries, where lattice curvature due to neighbor-neighbor accommodation can produce viable nuclei of an orientation related to the parent grains. For example, it is supposed that a deformed grain of {111}<110> orientation can have material rotated toward {554}<225> in the vicinity of its grain boundary.[20,21] An alternative version, which is supported by extensive metallography, is based on the work of Tse et al.,[22,23] who showed that orientation splitting of material belonging to the γ fiber can give rise to deformation or kink bands, which can also provide the essential lattice curvature for viable nucleation. The absence of metallographic information from bcc MgLi indicates that further discussion is not justified.

Clearly, the α-fiber is destroyed by recrystallization (Figures 8(a) and (b)) in the cold-rolled annealed hot band, as it is in the as-received cold-rolled hot band. It appears to be replaced by a string of orientations linking {100}<012> to the nearest {111}<123> component. This string of orientations is quite common in annealed low-carbon and IF steels. For example, for IF steel, a weak version is found after warm rolling to 75 pct followed by annealing at 710 °C[24] in annealed 95 pct cold-rolled material,[14] and in annealed material warm rolled 75 pct followed by cold rolling to 20 pct.[24] Figure 10(a) is taken from Reference 14 and shows this latter result. The origins of these recrystallization texture components lie in the spread of orientations in the α components caused by orientation splitting in IF steel,[14] and it is probable that bcc MgLi behaves similarly.
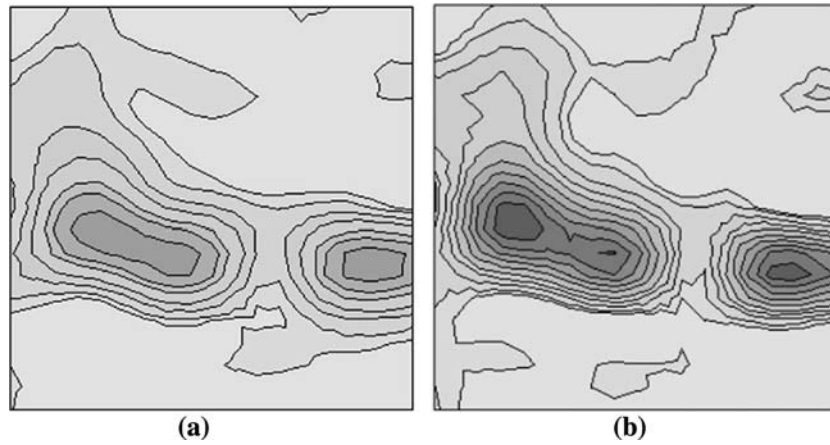
Fig. 10—$\phi_2$ 45 deg sections of the ODFs of IF steel. (*a*) Warm rolled 75 pct followed by cold rolling an additional 20 pct and annealing at 710 °C taken from Ref. 14. Intensities: 1, 2, 4, 6, 8, 11, and 14 (maximum 16.3). (*b*) Same material annealed at 850 °C, taken from Ref. 24. Intensities: 1, 2, 4, 6, 8, 11, 14, 17, 20, and 23 (maximum 25.95).

Increasing the annealing time to 15 minutes allows grain growth (a grain-boundary-curvature driven process) to occur, and the texture changes from that shown in Figure 8(e) to that in Figure 9(e). Figure 10(b) taken from Quadir *et al.*[24] shows a very similar spread. It seems that components at the edges of the spreads of the major recrystallization components increase in importance during grain growth. This is reasonable, since material at the centers of the spreads would be orientation pinned, thus allowing the orientations at the edges of the spreads to grow into the major components. The near $\{111\}<123>$ components, (557) $[27\ \overline{41}\ 10]$, (111)$[1\ \overline{3}\ 2]$, and (665)$[\overline{10}\ \overline{25}\ 42]$, lie within the spread of the main recrystallization component, $\{554\}<225>$, and gain in prominence in the grain growth phase, *cf.* Figures 8(e) and 9(c). The $\{100\}<012>$ strengthens during grain growth, *cf.* Figures 8(e) and 9(c). The behavior of warm-rolled IF steel shown in Figure 10(b) shows a slight increase in ~$\{100\}<014>$, but it is not as pronounced as in the corresponding ODF for bcc Mg Li (Figure 9(c)). The behavior of the as-received hot band subject to grain growth is similar to the material in the annealed state, with the observation that the former has a higher effective rolling reduction, which affects the rolling, annealing, and grain growth textures by making them all relatively sharper, *e.g.*, compare Figures 2, 3, and 9(a) through (c) with Figures 9(d) through (f).

## C. *Prospects for Formability of Bcc MgLi Alloys*

The presence of near $\{100\}$ components in the recrystallized texture ($\{100\}<012>$) will seriously affect drawability and lead to a reduction in the Lankford parameter.[25] It is thus probable that, if the surface reactivity problem can be solved, the best that can be hoped for is the production of a randomly textured material, in which case the Lankford parameter will be unity. This can be achieved by the process giving rise to the ODF shown in Figure 9(d) or (e), for it is clear that an intermediate rolling reduction gives rise to more random textures.

## V. CONCLUSIONS

The behavior of bcc MgLi has been investigated as a candidate flat-rolled product with the idea of producing a light formable sheet metal. The main findings are as follows.

1. The rolling textures are very similar to other bcc metals such as IF steel, ferritic stainless steel, and Fe-3 pct Si when they are similarly processed. There is a fully formed $\alpha$ fiber centered on ~$\{100\}<110>$ and a $\gamma$ fiber centered on $\{111\}<110>$. A new fiber is formed ($\{100\}$//RP) with a peak in common with the $\alpha$ fiber $\{100\}<011>$ and other peaks at $\{100\}<014>$. These results indicate that bcc MgLi is behaving as a high SFE alloy.
2. The primary recrystallized textures have $\{554\}<225>$ and $\{100\}<012>$ components after rolling to 90 pct.
3. The grain growth textures are near $\{111\}<123>$, which is within the spread of the major recrystallization textures $\{554\}<225>$ and $\{100\}<012>$, and these strengthen over their levels obtained following primary recrystallization.
4. It is unlikely that a Lankford parameter greater than unity can be achieved in this bcc alloy.

## REFERENCES

1. W.A. Freeth and G.V. Raynor: *J. Inst. Met.*,1954, vol. 82, pp. 569–74.
2. I.J. Polmear: *Light Metals*, 3rd ed., Butterworth and Heinemann, Oxford, 1995.
3. T. Leffers: *Phys. Status Solidi*, 1968, vol. 25, pp. 337–45.
4. T. Leffers: *Text. Res. Pract.*, 1968.
5. R.E. Smallman and D. Green: *Acta Metall.*, 1964, vol. 12, pp. 145–54.
6. I.L. Dillamore and W.T. Roberts: *Metall. Rev.*, 1965, vol. 10, pp. 271–80.
7. D. Raabe and K. Lücke: *Scripta Mater.*, 1992, vol. 26, pp. 1221–26.
8. S. Mishra, C. Därmann, and K. Lücke: *Metall. Trans. A*, 1986, vol. 17A, pp. 1301–12.
9. D. Schläfer and H.J. Bunge: *Texture*, 1974, vol. 1, pp. 157–67.
10. H. Saka and G. Taylor: *Philos. Mag. A*, 1981, vol. 43, pp. 1377–92.
11. K. Kitajima, Y. Aono, H. Abe, and E. Kuramoto: in *Strength of Metals and Alloys*, P. Haasen, V. Gerold and G. Kostorz, eds., Pergamon, Oxford, United Kingdom, 1979, pp. 965–71.
12. A.M. Russell, L.S. Chumbley, V.B. Gantovnik, K. Xu, Y. Tian, and F.C. Laabs: *Scripta Mater.*, 1998, vol. 39, pp. 1663–67.
13. M.R. Barnett and J.J. Jonas: *ISIJ Int.*, 1997, vol. 37, pp. 697–705.
14. M.Z. Quadir and B.J. Duggan: *Acta Mater.*, 2004, vol. 52, pp. 4011–21.
15. D. Raabe: *Mater. Sci. Technol.*, 1995, vol. 11, pp. 461–68.
16. G.I. Taylor: *J. Inst. Met.*, 1938, vol. 62, pp. 307–24.
17. H. Honeff and H. Mecking: *Proc. 5th Int. Conf. on Texture of Materials*, Berlin, Germany, 1978, pp. 265–71.
18. P. Van Houtte: *Mater. Sci. Eng.*, 1982, vol. 55, pp. 69–77.
19. W.B. Hutchinson: *Int. Met. Rev.*, 1984, vol. 29, pp. 25–42.
20. W.B. Hutchinson: *Acta Metall.*, 1989, vol. 37, pp. 1047–56.
21. T. Senuma and K. Kawasaki: *ISIJ Int.*, 1994, vol. 34, pp. 51–66.
22. Y.Y. Tse, G.L. Liu, and B.J. Duggan: *Scripta Metall.*, 2000, vol. 42, pp. 25–30.
23. Y.Y. Tse and B.J. Duggan: *Metall. Mater. Trans. A*, 2006, vol. 37A, pp. 1055–64.
24. M.Z. Quadir, K.T. Lam and B.J. Duggan: *Proc. Inst. Mech. Eng.*, 2004, vol. 218, Part C, pp. 631–39.
25. D.V. Wilson: *J. Inst. Met.*, 1966, vol. 94, pp. 84–93.